ORGANOMETALLICS

Article

pubs.acs.org/Organometallics

Kinetic Study of Carbophilic Lewis Acid Catalyzed Oxyboration and the Noninnocent Role of Sodium Chloride

Joel S. Johnson, Eugene Chong, Kim N. Tu, and Suzanne A. Blum*

Department of Chemistry, University of California, Irvine, California 92697-2025, United States

Supporting Information

ABSTRACT: In the present study, the oxyboration reaction catalyzed by IPrAuTFA in the presence and absence of NaTFA has been examined with kinetic studies, mass spectrometry, and ^{1}H NMR and ^{11}B NMR spectroscopy. Data from monitoring the reactions over the temperature range from 30 to 70 °C, the catalyst range from 1.3 to 7.5 mol %, and the NaTFA additive range from 2.5 to 30 mol % suggests a mechanism that involves rate-determining catalyst generation. Data from additive studies that replaced NaTFA with NaBARF (BARF = tetrakis[3,5-bis(trifluoromethyl)phenyl]borate) or Bu_4NTFA as an alternative additive suggest that catalyst quenching from residual NaCl remaining from a one-pot substrate synthesis/reaction method is the cause of this effect, despite the low solubility of this NaCl byproduct in toluene. Material produced through an alternative, sodium chloride-free substrate synthesis exhibited faster reaction rates, consistent with a change in rate-determining step that depended on the substrate synthesis route.

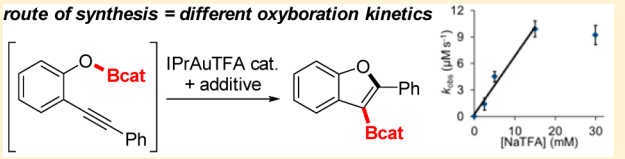

INTRODUCTION

Despite major progress in developing B−X element addition reactions to carbon−carbon π systems,[1−3] the corresponding B−O addition—oxyboration—remained unknown until it yielded to gold catalysis in 2014.[4] The role of the gold catalyst was proposed to be activation of the π system, a strategy orthogonal to other metal-catalyzed B−X σ-bond addition reactions which typically proceed through oxidative addition or σ-bond metathesis of the B−X bond (Scheme 1). This gold-catalysis working mechanistic strategy has since been successfully applied to B−N[5] and B−O[4,6] bond addition reactions to make organoboron heterocyclic building blocks; yet the rationale for the proposed pathway has been largely limited to analogy to existing carbophilic Lewis acid catalysis[7−12] rather than experimental observations (Scheme 1).[4] Additionally, the working mechanistic postulate for the oxyboration of alkynes included possible participation of trifluoroacetate (TFA) additive.

Scheme 1. Traditional Role of Metal Catalyst To Activate B−X Bonds vs New Role of Metal Catalyst To Activate C−C π Bonds, in B−X Addition Reactions to C−C π Bonds

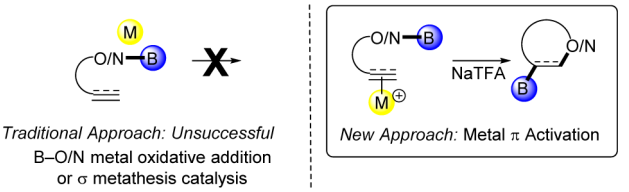

We herein investigate the kinetics of the gold-catalyzed oxyboration reaction in the synthesis of borylated benzofurans (eq 1) that serve as building blocks for the synthesis of

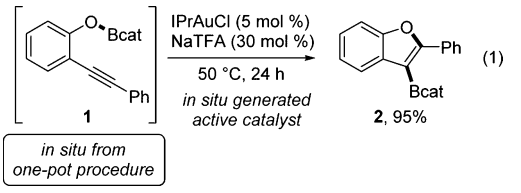

functionalized heterocycles. A practical feature of the originally reported method was the ability to generate the requisite B−O bond of the starting material from phenols and *B*-chlorocatecholborane (ClBcat) in one pot, without the need to isolate this moisture-sensitive intermediate. The kinetic data show consistency with the proposed carbophilic activation pathway but identify an unanticipated kinetic dependence on the reagents used and route of synthesis in the prior one-pot substrate-construction step. More specifically, the presence of NaCl generated during the one-pot substrate synthesis can be noninnocent to the reaction,[13] analogous to the reported silver salt effects on gold catalysis.[14−16] Similar to the case for silver halides, sodium chloride has a low solubility in organic solvents, yet we show that sufficient quantities remain in solution to influence reactivity. A possible explanation for the role of NaTFA additive as a chloride scavenger and transmetalation partner with gold chloride is thus provided herein. It is envisioned that these studies will assist in the development of methods for addition reactions of these previously recalcitrant B−X bonds to C−C π systems and thus enable rapid access to heterocyclic borylated building blocks for drug discovery and materials synthesis. Further, these studies may inform the

Received: November 10, 2015

 © XXXX American Chemical Society

DOI: 10.1021/acs.organomet.5b00939
Organometallics XXXX, XXX, XXX−XXX

development of dual-metal/metalloid catalytic chemistry for gold that currently requires halide-free conditions.[17]

RESULTS AND DISCUSSION

Carbophilic Lewis Acid Activation Mechanistic Proposal with Bifunctional Activation. The proposed mechanism for the oxyboration reaction in the synthesis of borylated benzofurans is shown in Scheme 2. The original mechanistic

Scheme 2. Proposed Mechanism for Oxyboration[a]

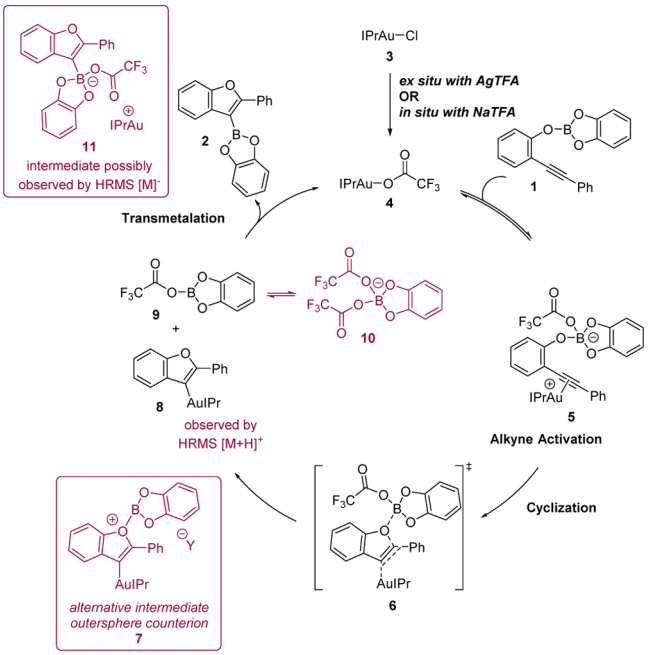

[a]Originally proposed structures in the catalytic cycle from ref 4 shown in black; additional data/possible intermediates from this work shown in purple (Y = BF_4, SbF_6, TFA).

hypothesis for oxyboration featured IPrAuTFA **4** as a bifunctional Lewis acidic/basic catalyst, in which the $IPrAu^+$ moiety participates in carbophilic Lewis acid activation of the alkyne in **1** and the TFA counterion coordinates to boron, to assemble intermediate **5**. Nucleophilic attack on the Au-activated C–C π bond with the TFA-activated B–O bond in **5**, through transition state **6**, generates organogold intermediate **8** and catB(TFA) **9**.[4] Subsequent Au-to-B transmetalation[17,18] between **8** and **9** affords the borylated benzofuran **2** and regenerates the IPrAuTFA catalyst. To our knowledge, our initial report of oxyboration was the first example of organogold to boron transmetalation;[4–6,17–19] the reverse reaction had been reported.[20–24] Given that the forward and reverse transmetalation reactions have both been reported, it seems plausible that small differences in the structure of the reagents affect which side of the transmetalation reaction is thermodynamically favored. Prior studies in our laboratory identified that some transmetalation systems with gold and boron are in equilibrium.[18]

Carbophilic Lewis Acid Activation Mechanistic Proposal without Bifunctional Activation. Alternatively, substrate **1** could be undergoing a carbophilic Lewis acid gold-mediated cyclization, wherein trifluoroacetate serves as an outer-sphere ion (eq 2). A nucleophilic attack of the oxygen lone pair to the IPrAu-activated C–C π bond could generate the key alternative intermediate organogold benzofuran/

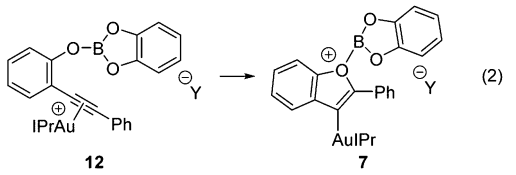

catechol borenium adduct **7**, which serves as a precursor to the borylated benzofuran product **2**. This pathway would be increasingly plausible with a less coordinating counterion on gold.[25–27] The counterion TFA is intermediate in coordinating ability, raising both possibilities.

Initial analysis of the reaction mixture of the oxyboration reaction in eq 1 prior to reaction completion by ESI-HRMS revealed the presence of molecular ion peaks consistent with the TFA-coordinated tetraborate component ($[M]^-$, m/z 425.0820) of intermediate **5**, or possibly in the cyclized intermediate **11**, and organogold intermediate **8** ($[M + H]^+$, m/z 779.3294). These initial findings suggested the viability of gold and trifluoroacetate intermediates in the oxyboration reaction, as proposed in Scheme 2; the simple detection of compounds, however, does not imply kinetic relevance. To probe the role of gold and the counterion, we therefore next determined the reaction order with respect to substrate **1**, gold catalyst, and trifluoroacetate, via kinetic studies of the transformation of **1** to **2** as described in detail in the following sections.

Kinetic Studies under Standard Conditions (NaCl Present). For the first set of kinetic experiments, we used the standard synthesis[4] of substrate **1** (eq 3) from the

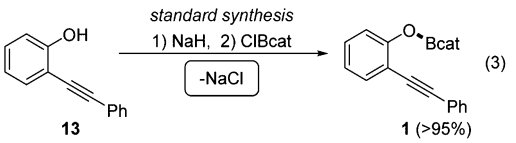

deprotonation of phenol **13** with NaH, followed by the reaction of the resulting sodium phenolate with ClBcat to eliminate NaCl byproduct and obtain **1** (>95%). A series of initial-rate kinetic experiments were conducted using ^{1}H NMR spectroscopy to monitor the formation of **2** with respect to time at 50 °C using the ERETIC method.[28] Error is reported as the standard deviation between triplicate runs.

For these kinetics experiments, one change was made in comparison to the previously reported synthetic procedure (of eq 1): the presumed active catalyst, IPrAuTFA **4**, was prepared ex situ via silver salt metathesis between IPrAuCl and AgTFA and then added to the reaction mixture, rather than producing it in situ via salt metathesis between IPrAuCl and NaTFA. This change was made to avoid convolution of the kinetic data via a concurrent catalyst generation step and to allow for the manipulation of known amounts of the anticipated active catalyst **4**. We discovered later, however, that speciation of gold was depended on substrate synthesis (vide infra) and that, therefore, the route of synthesis of each reagent would thus deserve additional scrutiny. In the absence of catalyst, no product formation occurred under otherwise identical conditions. This lack of conversion established that boron alone is insufficiently electrophilic to activate the alkyne toward nucleophilic attack in this system, perhaps in part because it contains three oxygen ligands.[6,29–31]

Consistent with the proposed mechanism (Scheme 2), the reaction exhibited a first-order kinetic dependence on the

DOI: 10.1021/acs.organomet.5b00939
Organometallics XXXX, XXX, XXX–XXX

concentration of added IPrAuTFA over the range of 1.3−7.5 mol % (Table 1, entries 1−4; Figure 1a).

Table 1. Oxyboration of 1 at Varied Concentrations of Catalyst and NaTFA: Investigation of Kinetic Order

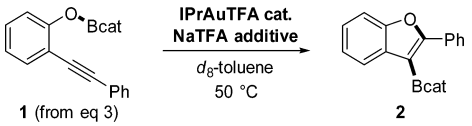

1 (from eq 3) 2

entry	IPrAuTFA (mol %)	NaTFA (mol %)	k_{obs} (μM s^{-1})
1	1.3	30	2.1 ± 0.3
2	2.5	30	5.5 ± 0.5
3	5.0	30	9.2 ± 1.1
4	7.5	30	11 ± 1.1
5	5.0	2.5	1.4 ± 0.7[a]
6	5.0	5.0	4.5 ± 0.6
7	5.0	15	9.9 ± 0.9

[a]The reaction is sufficiently slow that integration of small quantities of product produces a large error.

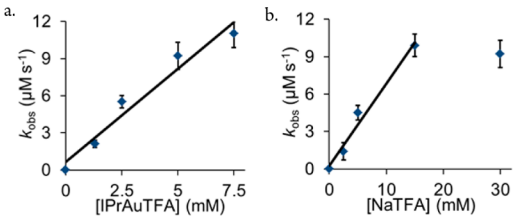

Figure 1. (a) Plot of zero-order k_{obs} (μM s^{-1}) vs [IPrAuTFA] showing first-order dependence. (b) Plot of zero-order k_{obs} (μM s^{-1}) vs [NaTFA] showing first-order dependence up to 15 mol %.

Monitoring of the chemical reaction kinetics over the course of the full reaction (Figure 2) indicated zero-order substrate

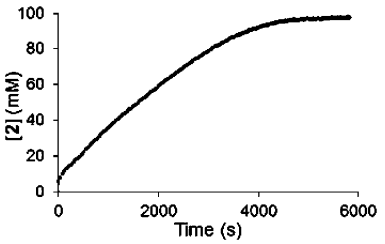

Figure 2. Plot of formation of **2** versus time using 7.5 mol % of IPrAuTFA and 30 mol % of NaTFA at 70 °C, showing a zero-order rate dependence on substrate concentration over the course of approximately 2 half-lives.

kinetics over the majority of the reaction (approximately 2 half-lives) and showed that initial-rate kinetic studies would provide information similar to that for the full course of the experiment. For this reason, initial-rate kinetics were then followed for the majority of the measurements.

Over this IPrAuTFA catalyst loading range (1.3−7.5 mol %), the reaction displayed these zero-order substrate kinetics in the presence of NaCl byproduct from substrate synthesis.[32] These saturation kinetics pinpointed a rate-determining step that did not involve catalyst−substrate binding.

Eyring Analysis. To gain additional insight into the rate-determining step, we examined the energetic parameters of the reaction. Rates measured over the temperature range of 30−70 °C with a fixed 7.5 mol % of IPrAuTFA and 30 mol % of NaTFA gave the activation parameters $\Delta H^{\ddagger}$ = 13 ± 2 kcal mol^{-1}, $\Delta S^{\ddagger}$ = −40 ± 5 cal mol^{-1} K^{-1}, and $\Delta G^{\ddagger}$ = 26 ± 2 kcal mol^{-1}. The large negative value of $\Delta S^{\ddagger}$ indicates a bimolecular rate-determining step. To maintain consistency with the observed zero-order substrate kinetics, this bimolecular step cannot involve substrate−catalyst binding. In the considered mechanisms, this data would be consistent with a rate-determining generation of the active catalyst from a precatalyst[33,34]—which would suggest that the active catalyst was not present from t = 0 after all—or with bimolecular recombination of **8** and **9** (Scheme 2).

Kinetic Dependence on NaTFA. In order to differentiate between these hypotheses, the kinetic dependence on the NaTFA additive was examined next. The reaction exhibited first-order kinetics with respect to NaTFA over the range of 0−15 mol % (Figure 1b). However, additional NaTFA after this point had no detectable effect on the rate. This absence of a consistent kinetic effect is seen through comparison of entries 3 and 7 in Table 1, showing similar k_{obs} values between 15 mol % of NaTFA (k_{obs} = 9.9 ± 0.9 μM s^{-1}) and 30 mol % of NaTFA (k_{obs} = 9.2 ± 1.1 μM s^{-1}). The observed first-order dependence on NaTFA from 0 to 15 mol % and non-first-order dependence at 30 mol % are possibly due to the low solubility of NaTFA in toluene at higher concentrations, which could produce similar effective concentrations of NaTFA under these two conditions. The data support the role of sodium, trifluoroacetate, or both in the rate-determining step.

To investigate the solubility and speciation of NaTFA in toluene under the reaction conditions, saturated solutions of NaTFA at 50 °C in toluene were examined by ^{19}F NMR spectroscopy. First, a saturated sample of only NaTFA in toluene was examined. This sample produced no observable signal in the ^{19}F NMR spectrum, indicating low solubility of this salt in the absence of other reaction components. Second, a sample was prepared identically, but with a stoichiometric quantity of starting material **1** present. In this case, sufficient TFA was solubilized for ^{19}F NMR detection, as observed by a small signal centered at δ −75 ppm that is within the range of literature values of compounds containing TFA.[35] Presumably the coordination of TFA to the empty p orbital on boron assists in its solubility in toluene, which could resemble the proposed double-activation intermediate **5**. The viability of coordination-assisted solubility of NaTFA was further supported in a simpler model system, wherein a solution of ClBcat and NaTFA in toluene at 50 °C produced sufficient quantities of $[(TFA)_2Bcat]^-$ **10** and $[(TFA)_4B]^-$ to be detected by MS (**10**, m/z 345; $[(TFA)_4B]^-$, m/z 463) with an isotopic pattern consistent with boron.

Thus, these results establish that trifluoroacetate can coordinate to boron as shown in intermediates **5** and **9**−**11**; however, the catalytic relevance of such species is not necessarily implied. In order to probe the catalytic relevance of such TFA-coordinated boron species, the kinetics of the reaction in the absence of added sodium, TFA, or both was next examined.

Kinetic Studies under Modified Reagent Conditions. In attempt to examine the accelerating effect of added NaTFA, a systematic variation of the additive was carried out (Table 2). Changing the cation of the trifluoroacetate additive from sodium (Table 2, entry 1) to tetrabutylammonium (Table 2, entry 2) resulted in no formation of **2**. Further examination of additives by substituting the TFA with the noncoordinating

DOI: 10.1021/acs.organomet.5b00939
Organometallics XXXX, XXX, XXX−XXX

Table 2. Variation of Additives and Its Effect on Oxyboration

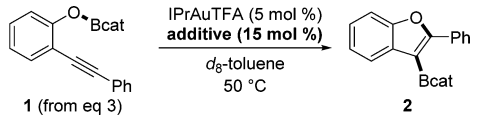

1 (from eq 3) 2

entry	additive	k_{obs} (μM s^{-1})
1	NaTFA	9.9 ± 0.9
2	Bu_4NTFA	no formation of **2**
3	NaBARF[a]	no formation of **2**
4	no additive	no formation of **2**

[a]BARF = tetrakis[3,5-bis(trifluoromethyl)phenyl]borate.

anion BARF (Table 2, entry 3), resulted in no formation of product. Importantly, no reactivity was observed with the presumed catalyst IPrAuTFA alone in the absence of additive (Table 2, entry 4), suggesting that catalyst inhibition was occurring from the beginning of the reaction, presumably by quenching the catalytically active $IPrAu^+$ species. It was evident that the NaTFA additive could play a critical role in overcoming such catalyst inhibition through scavenging residual chloride and/or serving as a transmetalation partner to regenerate the active catalyst, thus requiring further evaluation.

We considered the possibility that the presence of NaCl byproduct, generated during the preparation of **1** (eq 3), might have a detrimental effect on the reaction. As the IPrAuCl complex was previously shown to be an incompetent catalyst for this reaction,[4] we hypothesized that NaCl, although only limitedly soluble in toluene, might not be benign. It might cause catalyst inhibition from counterion exchange with the IPrAuTFA catalyst into the inactive IPrAuCl complex (eq 4), such that the rate-determining step under the reaction conditions was regeneration of the active catalyst.[33,34] We further hypothesized that the additional NaTFA[4,5] might be preventing this catalyst quenching by chloride through the common ion effect to push the equilibrium of eq 4 to the left to increase the concentration of the active IPrAuTFA catalyst. Hence, a chloride-free synthetic route to starting material **1** was examined next.

$$\underset{\text{active}}{\text{IPrAuTFA}} + \underset{\text{byproduct from } \mathbf{1}}{\text{NaCl}} \rightleftharpoons \underset{\text{inactive}}{\text{IPrAuCl}} + \text{NaTFA} \quad (4)$$

Change in Route of Synthesis of Substrate 1: Sodium Chloride-Free Generation. The treatment of **13** with 1 equiv of ClBcat (eq 5, top arrow), followed by removal of the HCl

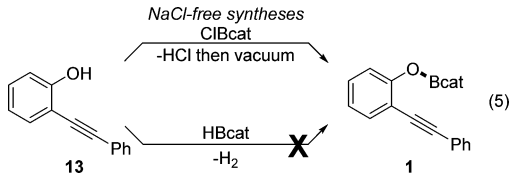

13 1

byproduct under vacuum, afforded **1** in quantitative yield via a route suitable for small-scale mechanistic experiments; This approach is less practical from a synthetic standpoint than the previous substrate synthesis due to the formation of corrosive HCl gas and the requirement to trap this gas under vacuum. Unfortunately, the exploration of an alternative synthesis of **1** from the reaction of **13** and HBcat (eq 5, bottom arrow) that could generate less corrosive hydrogen gas as the byproduct was unsuccessful.

With substrate **1** in hand using eq 5, the kinetics of NaCl-free oxyboration reaction was examined (Table 3). With 5 mol % of

Table 3. Oxyboration of NaCl-Free Generated Substrate 1 and the Effect of NaTFA Additive on This Reaction

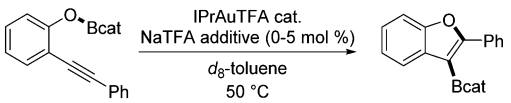

1 (from eq 5) *from NaCl-free synthesis* 2

entry	IPrAuTFA (mol %)	NaTFA (mol %)	k_{obs} (μM s^{-1})
1	0	0	no formation of **2**
2	5.0	0	54 ± 6
3	5.0	5.0	19 ± 1

IPrAuTFA catalyst alone in the absence of any additive, a significantly faster reaction rate for the formation of **2** was observed with k_{obs} = 54 ± 6 μM s^{-1} (Table 3, entry 2), in comparison to the rate observed with the previously reported NaCl-present conditions using 5 mol % of IPrAuTFA and the largest amount of additive, 30 mol % of NaTFA (k_{obs} = 9.2 ± 1.1 μM s^{-1}; Table 1, entry 3). These drastically different k_{obs} values observed between NaCl-free and NaCl-present conditions support the hypothesis that NaCl is indeed inhibiting gold catalysis, presumably due to the chloride quenching of the catalytically active $IPrAu^+$ species into inactive IPrAuCl.

Under the conditions of Table 3, the reaction no longer displayed zero-order substrate kinetics. This result was consistent with a change in rate-determining step such that the rate was no longer limited by catalyst generation.

In order to examine the kinetic dependence on substrate and catalyst concentration more clearly under NaCl-free conditions, the catalyst loading was varied from 0 to 1.25, 2.5, 5, and 7.5 mol % and the fit of the reaction kinetics was examined. Zero-, first-, and second-order kinetics did not fit the full reaction course (example, 2.5 mol % of catalyst, average of triplicate runs, Figure 3a). Specifically, the first-order assessment plot displayed a slight data curvature that deviated from the linear fit for both 2.5 and 5 mol % of catalyst Figure 3b,d). The second-order assessment plot deviated slightly at early reaction times with 2.5 mol % of catalyst but fit well for the full measured reaction course for 5.0 mol % (Figure 3c,e). Because the rate of product formation was slower than that required for a good fit at early times, these fits may imply a catalyst induction period. In the case of 7.5 mol %, wherein the reaction was sufficiently fast that initial rates were not measured, the kinetics best fit first order (see the Supporting Information for data and fits from 1.25 and 7.5 mol % catalyst). This deviation at early conversions precluded using initial rates to determine the order in the gold catalyst. In the absence of catalyst no product formation occurred (Table 3, entry 1).

Interestingly, the addition of 5 mol % of NaTFA additive under NaCl-free reaction conditions lead to a decreased reaction rate (k_{obs} = 19 ± 1 μM s^{-1}; Table 3, entry 3); under these conditions, the previously accelerating additive had a decelerating effect. The increased availability of TFA in solution may shift the equilibrium between the proposed species (TFA)Bcat **9** and $[(TFA)_2Bcat]^-$ **10** toward **10** (Scheme 2). The plausibility of such an equilibrium and proposal was supported by the detection of **10** by MS in a related model reaction between commercially available ClBcat, as a surrogate boron electrophile to (TFA)Bcat, and NaTFA. Therefore,

DOI: 10.1021/acs.organomet.5b00939
Organometallics XXXX, XXX, XXX−XXX

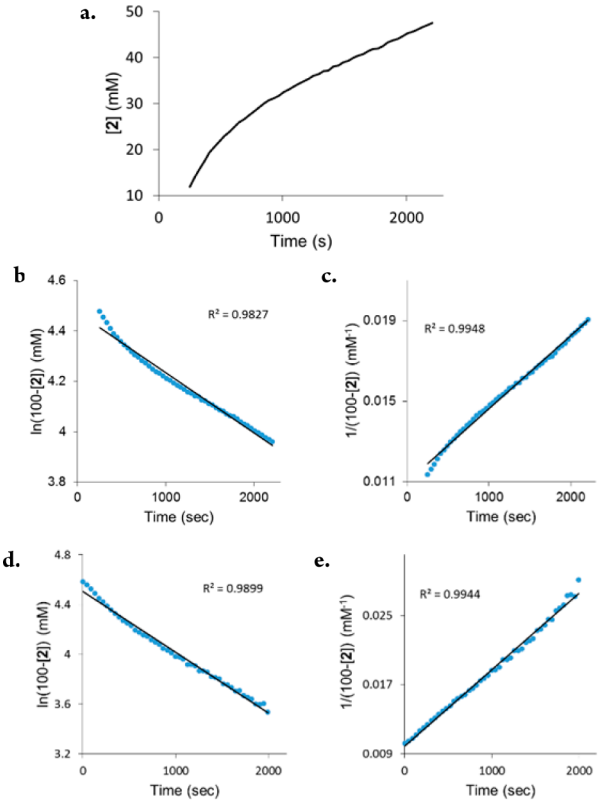

Figure 3. (a) Plot of formation of **2** versus time using 2.5 mol % of IPrAuTFA at 50 °C, showing a non-zero-order rate dependence on substrate concentration. (b) First-order fit plot with 2.5 mol % of catalyst. (c) Second-order fit plot with 2.5 mol % of catalyst. (d) First-order fit plot with 5.0 mol % of catalyst. (e) Second-order fit plot with 5.0 mol % of catalyst.

NaTFA additive is necessary to overcome catalyst inhibition by NaCl, but an additional 1 equiv of NaTFA respective to gold can impede catalysis.

Now that the role of NaTFA was established, we next probed whether the oxyboration reaction can also be catalyzed by carbophilic Lewis acid catalysis in the absence of assistance by TFA. For this study, substrate **1** was synthesized under NaCl-free conditions. Two other (NHC)gold(I) complexes with weakly coordinating counterions, IPrAu(NCMe)SbF_6 and IPrAu(NCMe)BF_4, were prepared using literature procedures.[36] These counterions would be less likely to coordinate to boron. These experiments were performed to assess the accessibility of a mechanism proceeding through intermediate **7**, which has no inner-sphere assistance in the B−O bond cleavage step from TFA.

Under NaCl-free conditions, the reaction mixture of **1** with these gold catalysts (5 mol %) were heated to 50 °C for 18 h (Table 4). The catalytic use of IPrAu(NCMe)BF_4 gave full conversion to product **2** under these conditions (Table 4, entry 2). These results indicated that the TFA counterion is not required for oxyboration, which suggests that carbophilic Lewis acid catalysis with $IPrAu^+$ species can mediate this reaction independent of TFA (Scheme 2 via intermediate **7**). In contrast, the reaction with IPrAu(NCMe)SbF_6 gave trace quantities of **2** (<5%) under the same conditions (Table 4, entry 3). Heating this reaction mixture at the higher temperature of 80 °C for 19 h resulted in the formation of **2** (77%), which is also consistent with a carbophilic Lewis acid

Table 4. Examination of Gold Catalysts with Varying Counterions

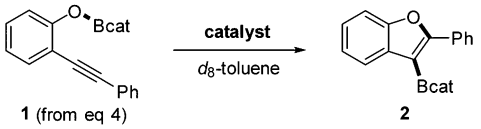

1 (from eq 4) **2**

entry	catalyst (5 mol %)	conditions	conversion (%)[a]
1	IPrAuTFA	50 °C, 18 h	>95
2	IPrAu(NCMe)BF_4	50 °C, 18 h	>95
3	IPrAu(NCMe)SbF_6	50 °C, 18 h	<5
4	IPrAu(NCMe)SbF_6	80 °C, 19 h	77
5[b]	IPrAu(NCMe)SbF_6	23 °C, 44 h	66

[a]Determined by ^{1}H NMR spectroscopy using 1,3,5-triisopropylbenzene as an internal standard. [b]20 mol % of NaTFA added.

catalyzed reaction (Table 4, entry 4). The differing reactivities observed between these two catalysts can be attributed to the lesser solubility of IPrAu(NCMe)SbF_6 in comparison to IPrAu(NCMe)BF_4, on the basis of qualitative assessment of the weaker intensity of IPr ligand signals in d_8-toluene for the former than for the latter complex in ^{1}H NMR spectra of these reaction mixtures.[37] Presumably, heating the reaction mixture to 80 °C allows for increased solubility of IPrAu(NCMe)SbF_6 in toluene for subsequent participation in the oxyboration reaction.

Furthermore, the catalytic activity of IPrAu(NCMe)SbF_6 was also revived, even at room temperature (Table 4, entry 5), upon the addition of 20 mol % of NaTFA (66% ^{1}H NMR spectroscopic yield of **2** in 44 h). This observation can be attributed to either NaTFA participating in the proposed bifunctional activation of the substrate **1**, as observed by the appearance of ^{11}B NMR spectroscopy signal at δ ~1 ppm in this sample that may correspond to tetraborate species, or simply acting as an agent that helps solubilize the catalytically active $IPrAu^+$ species for carbophilic Lewis catalysis.

Experimental results up to this point suggested that oxyboration of **1** could plausibly be catalyzed by bifunctional Lewis acid/base catalysis using IPrAuTFA and/or simply by carbophilic Lewis acid catalysis with the $IPrAu^+$ species alone. In order to compare these two proposed pathways, the reaction of **1** with 5 mol % of IPrAuTFA or IPrAu(NCMe)BF_4 was monitored side by side over time by ^{1}H NMR spectroscopy (Figure 4). In the first 380 min of the reaction at ambient temperature, the IPrAuTFA-catalyzed reaction (pale blue line) resulted in slightly faster formation of **2** in comparison to the IPrAu(NCMe)BF_4-catalyzed reaction (pale red line). Com-

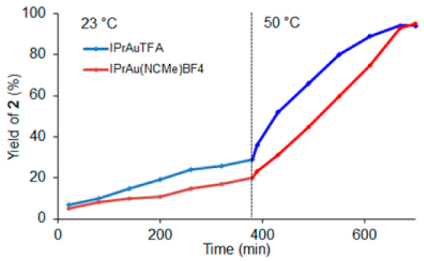

Figure 4. Monitoring the formation of **2** over time under NaCl-free conditions using IPrAuTFA (in blue) and IPrAu(NCMe)BF_4 (in red). Conditions: 23 °C from 0 to 380 min (in paler shade); 50 °C from 380 to 700 min (in brighter shade).

DOI: 10.1021/acs.organomet.5b00939
Organometallics XXXX, XXX, XXX−XXX

parable reactivity is observed between these two complexes when the temperature is raised to 50 °C for an additional 320 min of reaction time (blue and red lines between 380 and 700 min).

Given these results with chloride-free conditions, the catalysts with and without the possibility of Lewis base assistance display reactivity sufficiently similar for the conclusion that Lewis base assistance is not a requirement for oxyboration; nevertheless, the operation of such an assisted mechanism with the TFA counterion when it is present cannot be ruled out.

In the scenario that the oxyboration mechanism is indeed operated independently by carbophilic Lewis acid catalysis by $IPrAu^+$ species without the inner-sphere assistance of the counterion (Y^-), we propose that the reaction follows the revised pathway shown in Scheme 3. One possible transmetalation mechanism is that, after intermediate **12** undergoes IPrAu-catalyzed cyclization, the resulting two cyclized intermediates **7** could undergo intermolecular transmetalation to afford product **2** and regenerate the catalyst. While the concentration of two activated complexes might be low, analogous gold-activated cyclization intermediates have been observed by NMR to build up in other systems.[19] An alternative consistent mechanism that avoids the need to bring two activated molecules together involves intermediate **7** reacting with starting material **1** in a metal/metalloid transfer step. This alternative mechanism is also plausible.

Scheme 3. Revised Proposed Mechanism for Oxyboration

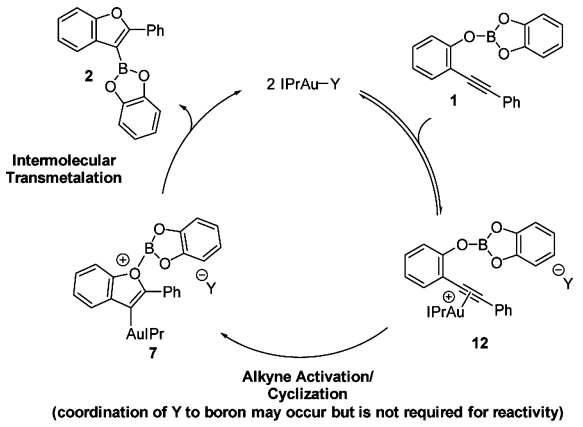

CONCLUSIONS

In conclusion, these results show that counterions capable of coordinating and activating boron in the carbophilic Lewis acid catalyzed oxyboration reaction are not required for oxyboration reactivity. A revised mechanism was proposed that maintains the original Au-catalyzed alkyne activation but does not require binding by the counterion. Kinetic measurements identified a dependence on the route of substrate synthesis. When residual sodium chloride was present, the catalyst was quenched, despite the low solubility of this ionic compound in toluene. However, chloride-induced catalyst inhibition of cationic gold can be circumvented by using the NaTFA additive, and its substoichiometric addition was beneficial to reviving the catalytic activity of gold. Determination of the noninnocent role of sodium chloride is expected to facilitate catalytic reaction development because sodium salts are increasingly attractive for late-metal catalyst generation, given that the alternative silver salts have already been established to be noninnocent. An understanding of the reaction mechanism for Lewis acid catalyzed oxyboration is similarly anticipated to assist in the development of new B–X addition reactions to alkynes and alkenes.

EXPERIMENTAL SECTION

General Considerations. All manipulations were conducted under a nitrogen atmosphere using a glovebox or standard Schlenk techniques unless stated otherwise. All chemicals were used as received from commercial sources unless otherwise noted. Sodium trifluoroacetate (NaTFA) was dried at 130 °C under vacuum (10 mTorr) for 24 h before use. Toluene, CH_2Cl_2, and Et_2O were purified by passage through an alumina column under argon pressure on a push-still solvent system. d_8-Toluene was dried over CaH_2, degassed using three freeze–pump–thaw cycles, and vacuum-transferred prior to use. ^1H, ^{11}B, and ^{19}F NMR spectra were recorded on a Bruker AVANCE-600 or Bruker DRX-400 spectrometer. All chemical shifts (δ) are reported in parts per million (ppm) and referenced to the residual proton solvent peak (δ 7.26 ppm for $CDCl_3$, δ 2.08 ppm for d_8-toluene in ^1H NMR spectra). ^{11}B and ^{19}F NMR spectroscopy experiments are referenced to the absolute frequency of 0 ppm in the ^1H dimension according to the Xi scale. Low- and high-resolution mass spectrometry data were obtained at the University of California, Irvine.

Synthesis of 2-(Phenylethynyl)phenol (13). A flame-dried 1 L round-bottom flask equipped with a stir bar was charged with 2-iodophenol (14.0 g, 63.6 mmol), CuI (1.09 g, 5.71 mmol), and $Pd(PPh_3)_2Cl_2$ (1.33 g, 1.89 mmol). In this flask, toluene (320 mL), diisopropylamine (8.90 mL, 63.6 mmol), and phenylacetylene (10.5 mL, 95.4 mmol) were added sequentially. The reaction mixture was stirred for 8.5 h at 25 °C. Ethyl acetate (100 mL) was added, and the organic layer was washed with saturated ammonium chloride solution (50 mL) and then brine (50 mL) and dried over sodium sulfate. The organic layer was filtered and concentrated, and the resulting dark brown oil was purified by flash chromatography (12% EtOAc in hexanes). The resultant oil was further recrystallized from hexanes to afford a brown crystalline solid (6.82 g, 55%). ^1H NMR (600 MHz, $CDCl_3$): δ 7.58–7.56 (m, 2H), 7.45 (dd, J = 7.6, 1.6 Hz, 1H), 7.40–7.39 (m, 3H), 7.31–7.28 (m, 1H), 7.02 (dd, J = 8.3, 0.8 Hz, 1H), 6.94 (td, J = 7.5, 1.0 Hz, 1H), 5.89 (s, 1H). This spectrum is in agreement with previously reported spectral data.[4]

Synthesis of IPrAuTFA (4). IPrAuCl (124 mg, 0.200 mmol) and AgTFA (44.2 mg, 0.200 mmol) were weighed in separate vials. IPrAuCl was dissolved in CH_2Cl_2 (1 mL), and this solution was transferred to the vial containing AgTFA. Additional CH_2Cl_2 (1 mL) was used to rinse the vial during the transfer. The vial was capped with a Teflon-coated cap and covered in aluminum foil, and the reaction mixture was stirred for 30 h in the glovebox. The resulting reaction mixture was then filtered through glass fiber filter paper. The filtrate was concentrated in vacuo to afford a colorless solid (110 mg, 79%). This complex was used without further purification, and its ^1H spectrum is in agreement with previously reported spectral data.[5] ^1H NMR (400 MHz, d_8-toluene): δ 7.13 (t, J = 7.8 Hz, 2H), 6.97 (d, J = 7.8 Hz, 4H), 6.30 (s, 2H), 2.47 (septet, J = 6.8 Hz, 4H), 1.36 (d, J = 6.8 Hz, 12H), 1.03 (d, J = 6.8 Hz, 12H).

General Procedure for the Preparation of Kinetic Experiment Samples. *Example Given for Standard Synthesis of* ***1*** *(Eq 3) and Subsequent Oxyboration Reaction using 7.5 mol % of IPrAuTFA and 30 mol % of NaTFA.* **13** (34.0 mg, 0.175 mmol), 89% NaH (4.7 mg, 0.18 mmol), *B*-chlorocatecholborane (27.0 mg, 0.175 mmol), and NaTFA (7.2 mg, 0.053 mmol) were weighed individually in separate dram vials. Substrate **13** was dissolved in d_8-toluene (250 μL) and transferred to the vial containing NaH. This mixture was stirred by shaking the vial by hand, allowed to sit for 15 min, and then transferred to the vial containing *B*-chlorocatecholborane. Additional d_8-toluene (2 × 250 μL) was used to rinse the first two vials during the transfer. The reaction mixture was allowed to sit for 30 min with occasional stirring by shaking the vial by hand. To this mixture was added NaTFA as a suspension in d_8-toluene (650 μL),

DOI: 10.1021/acs.organomet.5b00939
Organometallics XXXX, XXX, XXX–XXX

which gave the total volume as 1400 μL. From this boric ester stock solution, 400 μL was transferred to a J. Young NMR tube and capped with a rubber septum. This was repeated a total of three times to create three identical samples. To prepare the 7.5 mol % IPrAuTFA stock solution, the IPrAuTFA catalyst (9.2 mg, 0.013 mmol) was dissolved in d_8-toluene (350 μL).

*Example Given for NaCl-Free Synthesis of **1** (eq 5, Top Arrow) and Subsequent Oxyboration Reaction using 5 mol % of IPrAuTFA.* **13** (34.0 mg, 0.175 mmol) was dissolved in d_8-toluene (250 μL) and placed in a vial containing *B*-chlorocatecholborane (27.0 mg, 0.175 mmol). Additional d_8-toluene (250 μL) was used to rinse and transfer. The solution was allowed to sit for 20 min, and the HCl byproduct and solvent were removed under vacuum for 40 min. The resulting compound **2** was dissolved in d_8-toluene (1400 μL). From this boric ester stock solution, 400 μL was transferred to a J. Young NMR tube and the tube was capped with a rubber septum. This was repeated a total of three times to create three identical samples. To prepare the 5 mol % IPrAuTFA stock solution, the IPrAuTFA catalyst (6.1 mg, 0.0088 mmol) was dissolved in d_8-toluene (350 μL).

General Procedure for Kinetic Experiments. A J. Young NMR tube containing **2** (from the above procedure) and one gastight syringe with 100 μL of the IPrAuTFA solution, capped with a rubber stopper, were removed from the glovebox. The rubber septum on the J. Young NMR tube was wrapped in Parafilm. The sample in the J. Young NMR tube was immediately transported to the NMR spectrometer, which underwent temperature calibration before sample injection. The IPrAuTFA solution was injected using the gastight syringe into the J. Young NMR tube. This tube was shaken and inserted into the NMR spectrometer. Acquisition of spectra immediately followed. The acquisition time was set to 6 s. A 90° pulse was used. The line broadening was set to 1 Hz. There was one scan taken per experiment, and there were no dummy scans . A total of 50 experiments were conducted sequentially with 34 s delays between experiments.

Synthesis of Bu_4NTFA. The synthetic procedure was adapted from the literature.[38] Trifluoroacetic acid (0.04 mL, 0.5 mmol) was added dropwise into a 10 mL round-bottom flask containing trimethyl phosphate (0.7 mL, 6.0 mmol). To this stirred solution was added Bu_4NBr (161 mg, 0.500 mmol). The reaction mixture was stirred at 60 °C overnight. Excess trimethyl phosphate was removed via vacuum distillation at 85 °C. The resultant residue was dissolved in CH_2Cl_2 (2 mL), followed by addition of 25 drops of a 10% (w/v) NH_4OH aqueous solution. Once the pH of the solution was neutralized (pH 7), water (2 mL) was added. The organic layer was separated, and the aqueous layer was extracted with CH_2Cl_2 (2 × 2 mL). The combined organic layers were concentrated and dried under high vacuum at 100 °C overnight. The product was isolated as a beige solid (133 mg, 75%) and used without further purification. ^{1}H NMR (600 MHz, $CDCl_3$): δ 3.32−3.27 (m, 8H), 1.68−1.61 (m, 8H), 1.44 (sextet, *J* = 7.4 Hz, 8H), 1.01 (t, *J* = 7.4 Hz, 12H). ^{19}F NMR (376 MHz, $CDCl_3$): δ −75.1. These spectra are in agreement with previously reported spectral data.[38]

Synthesis of IPrAu(NCMe)BF_4. The synthetic procedure was adapted from the literature.[36] A dram vial equipped with a magnetic stir bar was charged with IPrAuCl (300 mg, 0.480 mmol) and $AgBF_4$ (94 mg, 0.48 mmol). In this vial was placed MeCN (2 mL), and the reaction mixture was stirred for 5 min. For workup, the reaction solvent was separated from the AgCl byproduct and concentrated in vacuo. The resulting crude residue was diluted in CH_2Cl_2 (2 mL) and filtered through a short plug of silica gel to remove residual silver salts. Additional CH_2Cl_2 (2 × 2 mL) was used to ensure complete elution of the product from the silica gel. After concentration of the filtrate in vacuo, the product was obtained as a white solid (340 mg, 99%). ^{1}H NMR (600 MHz, $CDCl_3$): δ 7.58 (t, *J* = 7.9 Hz, 2H), 7.37 (s, 2H), 7.35 (d, *J* = 7.8 Hz, 4H), 2.44 (septet, *J* = 6.9 Hz), 2.41 (s, 3H), 1.30 (d, *J* = 6.9 Hz, 12H), 1.25 (d, *J* = 6.8 Hz, 12H). This spectrum is in agreement with previously reported spectral data.[36]

Synthesis of IPrAu(NCMe)SbF_6. The synthetic procedure was adapted from the literature.[36] A dram vial equipped with a magnetic stir bar was charged with IPrAuCl (250 mg, 0.40 mmol) and $AgSbF_6$ (152 mg, 0.43 mmol). In this vial was placed MeCN (2 mL), and the reaction mixture was stirred for 5 min. Workup identical with that for the synthesis of IPrAu(NCMe)BF_4 was used to obtain the product as a white solid (344 mg, 99%). ^{1}H NMR (600 MHz, $CDCl_3$): δ 7.59 (t, *J* = 7.9 Hz, 2H), 7.36 (d, *J* = 7.8 Hz, 4H), 7.33 (s, 2H), 2.45 (septet, *J* = 6.9 Hz), 2.33 (s, 3H), 1.32 (d, *J* = 6.9 Hz, 12H), 1.25 (d, *J* = 6.8 Hz, 12H). This spectrum is in agreement with previously reported spectral data.[36]

Examination of Gold Catalysts with Varying Counterions Using NaCl-Free Synthesis of 1. *Preparation of **1**.* To a cooled solution of **13** (0.265 g, 1.36 mmol) in Et_2O (5 mL) at −78 °C in a 25 mL Schlenk tube was slowly added a solution of *B*-chlorocatecholborane (0.210 g, 1.36 mmol) in Et_2O (5 mL). The reaction mixture was stirred while it was warmed to room temperature for 1 h. The HCl byproduct and the solvent were removed in vacuo to quantitatively yield **1** as a yellow oil, which was directly used to prepare a 0.272 M stock solution of **1** in d_8-toluene using a 5 mL volumetric flask. ^{1}H NMR (600 MHz, d_8-toluene): δ 7.38 (dd, *J* = 7.7, 1.7 Hz, 1H), 7.24−7.20 (m, 2H), 6.99−6.97 (m, 1 H), 6.92 (td, *J* = 7.6, 1.7 Hz, 1H), 6.86−6.84 (m, 3H), 6.83−6.80 (m, 2H), 6.75 (td, *J* = 7.6, 1.2 Hz, 1H), 6.69−6.65 (m, 2H). ^{11}B NMR (193 MHz, d_8-toluene): δ 23.1. These spectra are in agreement with previously reported spectral data.[4]

General Procedure for Catalyst Screen. A dram vial was charged with the gold complex (0.0068 mmol, 5 mol %). In this vial were placed **1** (500 μL, 0.136 mmol, 0.272 M) and 1,3,5-triisopropylbenzene (11.0 μL, 0.0453 mmol) as an internal standard using a gastight syringe. The suspension was mixed and transferred to a J. Young NMR tube using a Pasteur pipet. The reaction was either kept at ambient temperature or heated at a specified temperature. The reaction was monitored by ^{1}H NMR spectroscopy over time by observing growing signals of the product: doublet centered at δ 8.35 ppm and multiplet centered at δ 8.14 ppm.

■ ASSOCIATED CONTENT

Supporting Information

The Supporting Information is available free of charge on the ACS Publications website at DOI: 10.1021/acs.organomet.5b00939.

Additional kinetic plots and NMR spectra (PDF)

■ AUTHOR INFORMATION

Corresponding Author

*E-mail for S.A.B.: blums@uci.edu.

Notes

The authors declare the following competing financial interest(s): US Pat. No. 9,238,661.

■ ACKNOWLEDGMENTS

This work was supported by a grant from the NIH (1R01GM098512-01) and by the University of California, Irvine.

■ REFERENCES

(1) Miyaura, N. Hydroboration, Diboration, Silylboration, and Stannylboration. In *Catalytic Heterofunctionalization*; Togni, A., Grützmacher, H., Eds.; Wiley-VCH: Weinheim, Germany, 2001; pp 1−45.

(2) Suginome, M. *Chem. Rec.* **2010**, *10*, 348−358.

(3) Barbeyron, R.; Benedetti, E.; Cossy, J.; Vasseur, J.-J.; Arseniyadis, S.; Smietana, M. *Tetrahedron* **2014**, *70*, 8431−8452.

(4) Hirner, J. J.; Faizi, D. J.; Blum, S. A. *J. Am. Chem. Soc.* **2014**, *136*, 4740−4745.

(5) Chong, E.; Blum, S. A. *J. Am. Chem. Soc.* **2015**, *137*, 10144−10147.

(6) Tu, K. N.; Hirner, J. J.; Blum, S. S. *Org. Lett.* **2016**, *18*, 480.

(7) Dorel, R.; Echavarren, A. M. *Chem. Rev.* **2015**, *115*, 9028−9072.

DOI: 10.1021/acs.organomet.5b00939
Organometallics XXXX, XXX, XXX−XXX

(8) Hashmi, A. S. K.; Frost, T. M.; Bats, J. W. *Org. Lett.* **2001**, *3*, 3769−3771.
(9) Hashmi, A. S. K.; Enns, E.; Frost, T. M.; Schäfer, S.; Frey, W.; Rominger, F. *Synthesis* **2008**, *2008*, 2707−2718.
(10) Zhang, Y.; Xin, Z.-J.; Xue, J.-J.; Li, Y. *Chin. J. Chem.* **2008**, *26*, 1461−1464.
(11) Hashmi, A. S. K.; Ramamurthi, T. D.; Rominger, F. *Adv. Synth. Catal.* **2010**, *352*, 971−975.
(12) Abbiati, G.; Marinelli, F.; Rossi, E.; Arcadi, A. *Isr. J. Chem.* **2013**, *53*, 856−868.
(13) Hirner, J. J.; Roth, K. E.; Shi, Y.; Blum, S. A. *Organometallics* **2012**, *31*, 6843−6850.
(14) Shi, Y.; Peterson, S. M.; Haberaecker, W. W.; Blum, S. A. *J. Am. Chem. Soc.* **2008**, *130*, 2168−2169.
(15) Lu, Z.; Han, J.; Hammond, G. B.; Xu, B. *Org. Lett.* **2015**, *17*, 4534−4537.
(16) Wang, D.; Cai, R.; Sharma, S.; Jirak, J.; Thummanapelli, S. K.; Akhmedov, N. G.; Zhang, H.; Liu, X.; Petersen, J. L.; Shi, X. *J. Am. Chem. Soc.* **2012**, *134*, 9012−9019.
(17) Hirner, J. J.; Shi, Y.; Blum, S. A. *Acc. Chem. Res.* **2011**, *44*, 603−613.
(18) Hirner, J. J.; Blum, S. A. *Tetrahedron* **2015**, *71*, 4445−4449.
(19) For transmetalation from gold to other metals, see ref 16 and: Shi, Y.; Roth, K. E.; Ramgren, S. D.; Blum, S. A. *J. Am. Chem. Soc.* **2009**, *131*, 18022−18023.
(20) Forward, J. M.; Fackler, J. P., Jr.; Staples, R. J. *Organometallics* **1995**, *14*, 4194−4198.
(21) Partyka, D. V.; Zeller, M.; Hunter, A. D.; Gray, T. G. *Angew. Chem., Int. Ed.* **2006**, *45*, 8188−8191.
(22) Partyka, D. V.; Zeller, M.; Hunter, A. D.; Gray, T. G. *Inorg. Chem.* **2012**, *51*, 8394−8401.
(23) Hofer, M.; Gomez-Bengoa, E.; Nevado, C. *Organometallics* **2014**, *33*, 1328−1332.
(24) Smith, D. A.; Roşca, D.-A.; Bochmann, M. *Organometallics* **2012**, *31*, 5998−5600.
(25) Strauss, S. H. *Chem. Rev.* **1993**, *93*, 927−942.
(26) Beck, W.; Suenkel, K. *Chem. Rev.* **1988**, *88*, 1405−1421.
(27) Krossing, I.; Raabe, I. *Angew. Chem., Int. Ed.* **2004**, *43*, 2066−2090.
(28) Akoka, S.; Barantin, L.; Trierweiler, M. *Anal. Chem.* **1999**, *71*, 2554−2557.
(29) Hansmann, M. M.; Melen, R. L.; Rudolph, M.; Rominger, F.; Wadepohl, H.; Stephan, D. W.; Hashmi, A. S. K. *J. Am. Chem. Soc.* **2015**, *137*, 15469−15477.
(30) Warner, A. J.; Lawson, J. R.; Fasano, V.; Ingleson, M. J. *Angew. Chem., Int. Ed.* **2015**, *54*, 11245−11249.
(31) Chen, C.; Kehr, G.; Fröhlich, R.; Erker, G. *J. Am. Chem. Soc.* **2010**, *132*, 13594−13595.
(32) Anslyn, E. V.; Dougherty, D. A. *Modern Physical Organic Chemistry*; University Science Books: Sausalito, CA, USA, 2006; p 396.
(33) Sanford, M. S.; Ulman, M.; Grubbs, R. H. *J. Am. Chem. Soc.* **2001**, *123*, 749−750.
(34) Rosner, T.; Pfaltz, A.; Blackmond, D. G. *J. Am. Chem. Soc.* **2001**, *123*, 4621−4622.
(35) Wang, F.-P.; Chen, D.-L.; Deng, H.-Y.; Chen, Q.-H.; Liu, X.-Y.; Jian, X.-X. *Tetrahedron* **2014**, *70*, 2582−2590.
(36) de Frémont, P.; Marion, N.; Nolan, S. P. *J. Organomet. Chem.* **2009**, *694*, 551−560.
(37) See the Supporting Information.
(38) Jeon, J. Y.; Varghese, J. K.; Park, J. H.; Lee, S.-H.; Lee, B. Y. *Eur. J. Org. Chem.* **2012**, *2012*, 3566−3569.

DOI: 10.1021/acs.organomet.5b00939
Organometallics XXXX, XXX, XXX−XXX